Application and modeling of VCSELs in direct modulated optical links

TAMÁS MAROZSÁK

University of Technology and Economics, Department of Broadband Infocommunication Systems
tamas.marozsak@mht.bme.hu

Keywords: VCSEL, direct modulation, dynamic range, laser model

Vertical cavity surface emitting lasers, VCSELs, are very important light sources in optical communications. Their characteristics are very close to high performance edge emitting laser characteristics with low distortion, high modulation bandwidth and high dynamic range. At the same time their price can be an order less thanks to the new technology. This paper introduces the unique properties and application of these lasers in high speed direct modulated optical links. A novel circuit model is also shown, which is capable to simulate the spatial effects, like diffusion and spatial whole burning, in these lasers.

The semiconductor laser is one of the most important devices in today's communications systems. The optical carrier can transfer several GHz bandwidth digital signal or any kind of analog signals in this bandwidth. Even simultaneous transmission of baseband digital and radiofrequency analog signals can be applied [1]. The advantages of optical transmission, like small attenuation, high bandwidth and immunity to electromagnetic interference are evident, but the high price of optoelectronic devices still prevent this technology from being widely used. Fortunately, the ever increasing user demands and the fast development of new technologies transform the expensive technologies to everyday ones fast.

The VCSEL (Vertical Cavity Surface Emitting Laser) is an important milestone on this way, as it cuts the price of laserdiodes drastically and brings optical systems like Fiber To The Home (FTTH) into reality. On the next pages the main characteristics, some measurement results and modeling of these lasers are shown. The mathematical method used in modeling is general, and can be applied in circuit simulation of problems in other technical fields as well.

VCSEL structure

VCSELs carry the most important structural difference to conventional edge emitters in their names. The laser cavity is not a planar, but a vertical structure in the semiconductor wafer as shown in *Fig. 1.* As a consequence, this laser emits the light vertically to the surface. This is a very important feature in practice, because for testing the laser operation cutting of the semiconductor crystal is not needed as before. The individual lasers can be tested right after finishing the wafer because cutting of the semiconductor crystal is no longer needed for testing the laser. Cutting has no effect on the laser operation and therefore packaging or integration with other circuit elements is much easier.

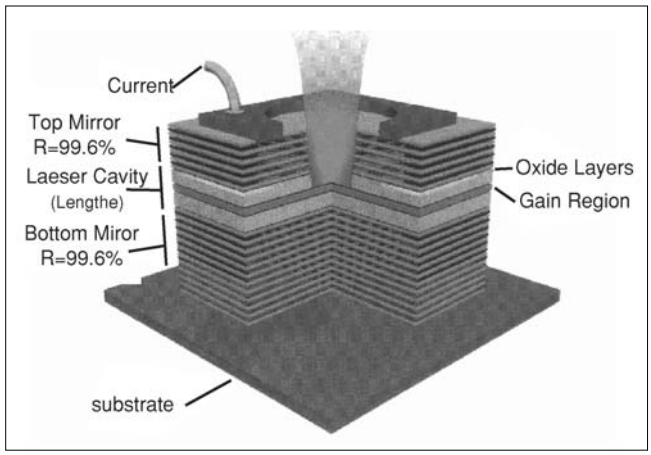

Fig. 1 Vertical structure of VCSELs

The structure of the vertical resonator is significantly different from the planar structure of edge emitters. The length of the resonator is defined by the thickness of some semiconductor layers grown on top of one other, and therefore it cannot be long: it falls into a few micron range. On such a small distance the round trip optical gain is small, therefore over 99% reflection is needed at the mirrors. Such a high value can only be made by distributed brag reflectors (DBR), which are formed by growing quarter wavelength thin layers having different refractive indeces on one other. To realize the required reflection, 20-30 layers are needed both at the bottom and the top. This layer structure is usually acchieved with molecular beam epitaxy (MBE). The active region between the mirrors usually consists of 1-2 quantum wells whose thickness is in the 10 nm range.

The number of layers in the mirrors is determined by the refractive index difference between the adjacent layers. The higher the difference, the smaller number of layers is needed. This is the reason why mostly 850-980 nm VCSELs are available. These lasers are made in the GaAlAs material system where sufficient refrac-

tive index difference can be achieved. This is not the case with InGaAsP, which is the material system for the 1300 és 1550 nm lasers.

There are some long wavelength VCSELs available, but this is still an intensive research area because the single mode fiber transmission systems require this wavelength. Therefore VCSELs are used mainly in multimode optical transmission systems where the dispersion limits the bandwidth seriously. The best wavelength optimized multimode fibers provide about 0.5 GHz·km, which is far less than the single mode fiber capacity. But it is inexpensive and many applications can work with this limited capacity. The optical bus can be mentioned as a good example, where several VCSELs are integrated into an array, therefore their light is easy to couple into a plastic fiber ribbon cable, and at the receiver side a Si photodiode array integrated with receiver circuits can detect the intensity at high speed.

Continuing the structure description, it is important to mention the transversal (parallel to the surface) properties. The cavity is a cylinder whose boundary is determined by the mirrors in the longitudinal direction but not in the transversal (radial) direction. In the beginning this boundary was created simply by disk shaped current injection as in the case of stripe lasers. The complex refractive index changes significantly where the current density is very high and this index difference from the surrounding material created the boundary and confined the optical field into the cavity. In this way only relatively large active diameter can be achieved, therefore an insulating oxide window is put into the structure, as shown also in Fig.1., to enhance the carrier confinement. In this layer a very small diameter hole can be realized, which means a very small resonator radius. The radial size of the cavity is important because it determines the number of possible transversal modes in the cavity. The intensity profile of the different transversal modes can be described by Bessel functions in a cylindrical coordinate system. The modes are denoted as $LP_{m,n}$, where the *m* and *n* indices refer to the number of periods in φ and *r* directions. *Fig. 2.* shows some of the lowest order modes in such a cavity.

The small radius and thickness of the active region causes very low threshold current compared to the edge emitting lasers. Typical values are less than 1mA and its variation is also significantly smaller. Another consequence of the small resonator length is that the longitudinal modes fall very far from each other in frequency and therefore only one of them can operate in the laser. Hence, the optical field has one longitudinal and more transversal modes in VCSELs.

This multiple transverse mode operation serves with some new interesting effects. The carrier density varies in space according to the optical field intensity. Where the intensity of a mode is high, the carrier density becomes locally low, which is called spatial hole burning (SHB). The dynamic evolution of these holes has fundamental effects on the VCSEL's static and dynamic characteristics. This will be explained better by simulation results later in the paper.

Single mode VCSEL can be fabricated by making a very small diameter oxide window. In this case the current density is very high in the cavity, which makes very high local heating. Because of this thermal problem, single mode VCSELs usually have small output power and therefore are not preferred. There are efforts to overcome this limitation, for example width fabricating mode selective mirror on the top of the laser. Recently 6mW output optical power was realized this way in a single mode device [2].

Modulation experiments

In short optical links the direct modulation of lasers gives the highest dynamic range [3]. In order to find this dynamic range, experimental investigations of laser diodes are needed. The bottom of the dynamic range is determined by noise and the upper limit is determined by nonlinear distortion.

The main source of noise in an optical link is the laser while the optical loss is not enough to attenuate it below the thermal noise in the receiver. This limit is generally 10dB optical loss in practice [3]. Therefore, in many cases the dynamic range is determined by the optical source itself.

The nonlinear distortion is not so important in digital transmission, but in analog transmission it has significant importance. The modulation depth cannot be increased over a limit in order to increase the signal to noise ratio because the second and third order intermodulation distortion (IMD) will degrade the performance. Cable television is a typical example where many channels are transmitted at the same time.

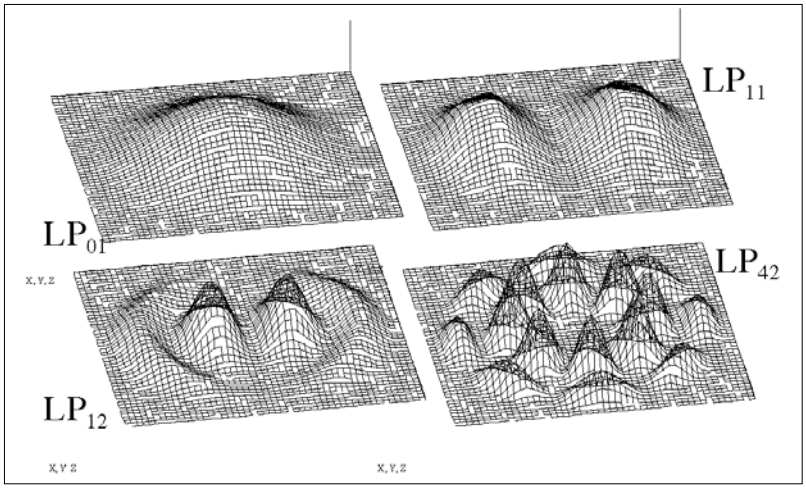

Fig. 2. Intensity mode profile of some fundamental modes in VCSELs

This is extremely sensitive for third order intermodulation because with increasing the power in the channels the third order IMD products increase according to the third power and rises over the noise level quickly. Therefore, a usual way to give the dynamic range of a device is to measure the difference between the output noise power and the signal power when the third order IMD product equals with the noise in a two-tone measurement. This parameter is called spurious free dynamic range, SFDR, and its unit is dB/Hz$^{3/2}$.

Such two-tone SFDR measurements were performed on conventional 1300 nm edge emitting lasers and on 850 nm VCSELs. The different operating wavelengths did not allow using the same photodiode. On 1300 nm single mode fiber, while on 850 nm multimode fiber was used. These differences were important because the same optical reflection level could not be ensured, which would be important to get consistent results, because the optical reflection affects the dynamic behavior of semiconductor lasers significantly. One of the edge emitting lasers was a Fabry-Perot, the other a DFB type, both fabricated on the same technology using multiple quantum wells.

The measurement results are shown in *Fig. 3.*, where the SFDR can be seen versus the modulating frequency. The main nonlinear effect in lasers is the relaxation oscillation, and approaching its characteristic frequency both the noise and the nonlinear distortion increases. Therefore we got decreasing dynamic range with increasing frequency. This indicates that high relaxation oscillation frequency can be important even in lower frequency applications.

Fig. 3. Measured dynamic range of different lasers

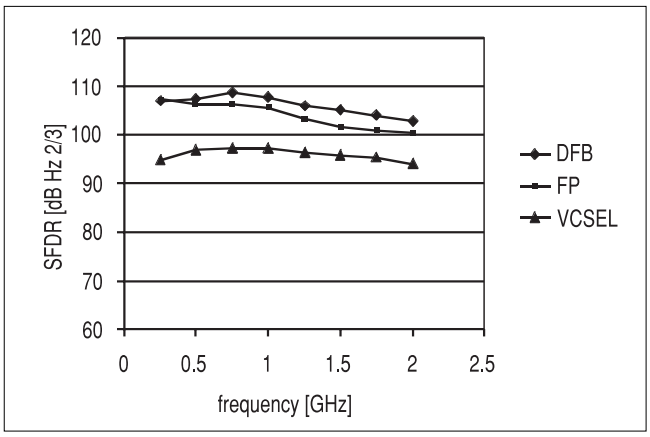

The optical reflection degrades the modulation performance. Even low level reflection causes increase and frequency peaking in noise and IMD. *Fig. 4.* shows measured results on 1300 nm Fabry-Perot lasers. The situation with VCSELs is similar but because the operating wavelength is 850 nm, the solution is more difficult because isolators for that wavelength are not available. The measurement showed that approximately 40 dB reflection loss is needed to make the laser operate near to its maximum dynamic range.

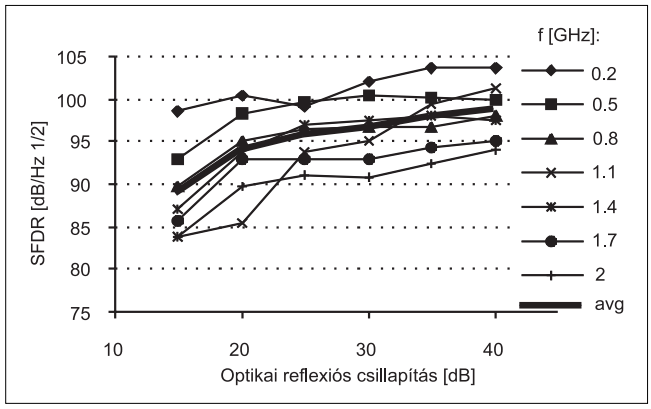

Fig. 4. Effect of optical reflection on the laser dynamic range

This could not be ensured in the VCSEL measurements in Fig. 3., therefore the real dynamic range should be higher than that shown in the diagram. Higher values are also reported in the literature [4]. In our case the dynamic range was smaller than the edge emitter's, but the measured 95 dB/Hz$^{3/2}$ value can be enough for most applications. For example the IEEE802.11b standard (wireless LAN) needs 94 dB at 2.5GHz [5], while a generic personal communication system, PCS, using $\pi/4$ DQPSK needs 72-83 dB/Hz$^{3/2}$ at 1900MHz [6].

Modeling of VCSELs

The accurate modeling of VCSELs based on the rate equations differs from the modeling of edge emitters. (In homogeneous medium the propagation of light can be derived by the Maxwell equations. In active medium containing free carriers the light effects are usually described by the rate equations. These can be derived from the Maxwell equations as well, but can be obtained by heuristics also by investigating the interactions between photons and free carriers. – *Editor's remark)*

Because these lasers operate in one longitudinal but more transversal modes, it is important to take the spatial processes into account. To simulate the spatial hole burning, it is essential to know the spatial distribution of the carrier density.

This means that in the rate equations the carrier density, in contrast with edge emitting lasers, can not be a scalar number but a function of space. The spatial distribution of the optical field is also different in the different modes as it was shown in Fig. 2. Therefore, the spatial dependence of the optical field also has to be taken into account. This can be done by writing separate rate equations for each modes using the modal gain theorem [7].

Finally, the following rate equations can be written:

$$\frac{dn_e(t,\underline{r})}{dt} = \frac{i(t,\underline{r})}{q} - \frac{n_e(t,\underline{r})}{\tau_e} - v_g \cdot g(t,\underline{r}) \cdot n_p(t,\underline{r}) \qquad (1)$$

$$\frac{dN_{p,i}}{dt} = v_g \cdot g_i \cdot N_{p,i} + \beta \cdot \frac{N_e}{\tau_e} - \frac{N_{p,i}}{\tau_p} \tag{2}$$

where n_e is the carrier density, t is time, $\underline{r}$ is the space vector, i is the pumping current, q is electron charge, τ_e is average electron lifetime, v_g is group velocity, g is optical gain, n_p is photon density, $N_{p,i}$ is the number of photons in the ith mode, g_i is the modal gain of the ith mode, β is the spontaneous emission factor, τ_p is average photon lifetime and N_e is the carrier number in the active region and can be expressed by n_e. $g(t,\underline{r})$ and g_i can be expressed by $n_e(t,\underline{r})$ and $n_p(t,\underline{r})$, and $n_p(t,\underline{r})$ can be obtained from the mode profiles and $N_{p,i}$. Index i means that we have as many photon rate equations as many optical modes are possible. This system of equations can be solved numerically after discretization of space. But it is computationally demanding, so difficult analyses like intermodulation takes very long time. Therefore I looked for a solution method, which does not has this drawback.

Circuit simulators solve systems of differential equations very efficiently. In addition it is very easy to choose between different types of analysis such as DC, AC transient or harmonic balance (for mixing and intermodulation) analysis. Therefore, I developed the circuit equivalent of these equations to simulate the main characteristics of VCSELs.

The main difficulty to overcome is that in circuit simulations only time or frequency can be the independent parameter, but in equations (1) and (2) both time and space are independent variables. The idea in eliminating this contradiction is that the optical intensity distribution of modes (the mode profiles) can be known a priori and they are not time dependent. The same can be done with the carrier density, it can be expressed as a linear combination of a limited series of orthogonal functions:

$$n_e(t,\underline{r}) = \sum_j n_{e,j} \cdot \Phi_j(\underline{r}) \tag{3}$$

where $\Phi_j(\underline{r})$ are given space functions and $n_{e,j}$ are their time dependent amplitudes. In this way the spatial dependence is represented by changing only the amplitudes of the different carrier density base functions. The space vector $\underline{r}$ can be changed to a simple radial coordinate, because the active region is very thin and therefore the carrier density does not change in vertical direction. The angular dependence can also be neglected for simplicity.

If the $\Phi_j(r)$ functions are orthogonal, then the electron equations (1) can be separated to j individual equations. For that (1) must be multiplied by each $\Phi_j(r)$ base function and integrated over the active volume. In the result only time varying amplitudes and space dependent integrals will remain. These integrals depend only on structural parameters, which are constants, and therefore these can be calculated in advance, and then any simulation can be carried out a number of times.

Doing all the derivations we obtain such a system of equations which consists of i photon and j electron equations, and mathematically independent of time:

$$\frac{dN_{p,i}}{dt} = v_g \Gamma_z a N_{p,i} \left(\sum_j n_{e,j} g_{ij} - n_t \right) + \beta \cdot \frac{N_e}{\tau_e} - \frac{N_{p,i}}{\tau_p} \tag{4}$$

$$\frac{dn_{e,J}}{dt} = \frac{I \cdot c_J}{q \cdot B_J} - \frac{n_{e,J}}{\tau_e} - \frac{v_g a}{\pi L B_J} \cdot \sum_i \sum_j n_{e,j} \cdot N_{p,i} \cdot g_{i,j,J} + \frac{v_g a \cdot n_t}{\pi L B_J} \sum_i N_{p,i} g_{i,J} \tag{5}$$

Here $g_{i,j}$ and $g_{i,j,J}$ constants are the results of spatial integrals which are called overlap integrals as they refer to the spatial overlap between the ith optical mode and jth electron distribution function. c_J are similar constants and B_J are normalizing constants. L is the length of the resonator, Γ_z is the longitudinal confinement factor, a is the gain constant (differential gain). The equations must be solved for $N_{p,i}$ and $n_{e,J}$, which are the time dependent amplitudes of the predefined distribution functions.

Fig. 5. Equivalent circuit for solving the multimode VCSEL rate equations

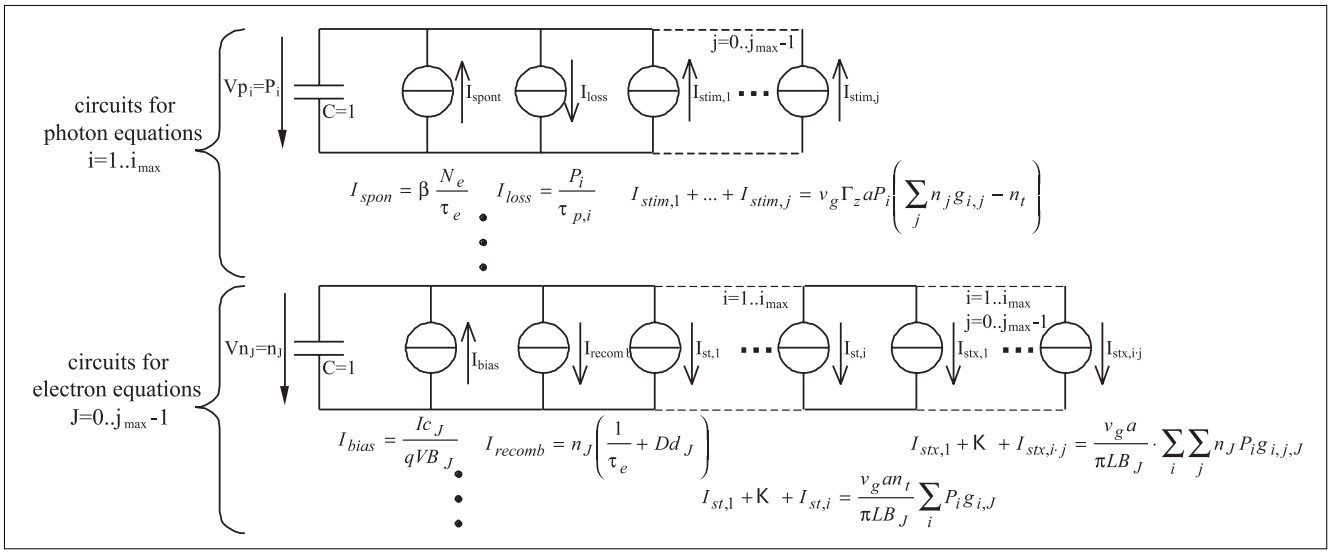

Carrier diffusion is also very important in VCSELs, therefore it has to be taken into account in the model. The electron rate equation, Eq. (1), must be extended by the term $+D\nabla^2 n(t,r,\varphi)$, where D is the diffusion constant, ∇ is the Laplace operator. If the $\Phi_j(r)$ carrier distribution functions are defined suitably, only the carrier rate equation will change by adding a $-n_{e,J}/(\gamma_J/R)^2$ term. γ_J and R are constants defined by the structure and material of the laser.

This idea to make the rate equations spatially independent can be found first in [8]. Later publications used this idea as well, but only for more simple cases and in many cases with not accurate mathematics.

The electrical equivalent of (4) and (5) can be derived as follows. The equations have the form similar to

$$C\frac{dV}{dt} = I_1 + I_2 + \ldots \text{ (assuming C=1)},$$

which is the Kirchoff equation for a circuit consisting of one capacitor and several current sources connected parallel. The photon number and the carrier density ($N_{p,i}$ and nJ in the equations) can be represented by the voltage on the capacitor, and the rates can be represented by the currents.

Using this idea, the equations can be modeled by the equivalent circuit network shown in *Fig. 5.* This electrical network consists of several subcircuits described above. There are i_{max} subcircuits for representing the i_{max} number of photon equations and j_{max} subcircuits representing the j_{max} number of electron equations. Each circuit contains one capacitor and a number of voltage controlled current sources equal to the number of terms on the right side of the equations. These terms are indicated in Fig. 5 below the generators. In these definitions the names of currents refer to the physical process that they represent. I_{stim}, I_{st} and I_{stx} mean different stimulated emission rate terms, the other names are obvious. In each subcircuit these currents are different as they are defined by constants having different i or J indices. In the expressions P_i and n_J become control voltages measured on the capacitors of the appropriate subcircuits (Vp_i and Vn_J). The input signal of the electrical network is given by I, which is common for the current sources defined by Ic_j/qdB_j in each electron subcircuit. In the simulation the network is solved for voltages Vp_i and Vn_J, which represent the number of photons, P_i, in the given mode and the electron density function amplitudes, n_J, respectively.

The method shown above for eliminating spatial dependence and creating the circuit equivalent was applied for VCSEL rate equations. But the principle is general and can be used to solve other problems as well.

The validity of the model and the circuit equivalent were checked by comparison to other models. The COST 268 action of the European Union had an open forum for comparing simulation results obtained from the same input parameters. The physical parameters of the laser for the following simulations were chosen from the modeling exercise of the action [9].

The simulations were done in APLAC, where using FOR statement arbitrary size ladder network can be defined in a few rows. The inputs of the simulation are material constants, parameters of the laser structure j_{max}. From these the $g_{i,j}$ and $g_{i,j,J}$, c_J és B_J constants are calculated, and then any type and any number of simulations can be carried out. In the following simulations two optical modes were supposed and j_{max}=11 was chosen giving rather accurate results.

Static characteristics, DC analysis

Fig. 6. shows the result of DC simulations in several bias points sweeping from 0 to 400 µA. It can be seen that lasing starts at I_{th} = 93 µA with the LP_{01} mode. As the optical intensity increases in this mode, a hole is created in the carrier distribution at r=0, as shown in *Fig. 7.* This affects the start of LP_{11} mode at I = 256 µA. Fig. 7 also shows that diffusion causes high electron density outside the r_i=3µm current aperture, which is also important in starting the LP_{11} mode.

Fig. 6. Result of DC simulation, bias current vs. optical power

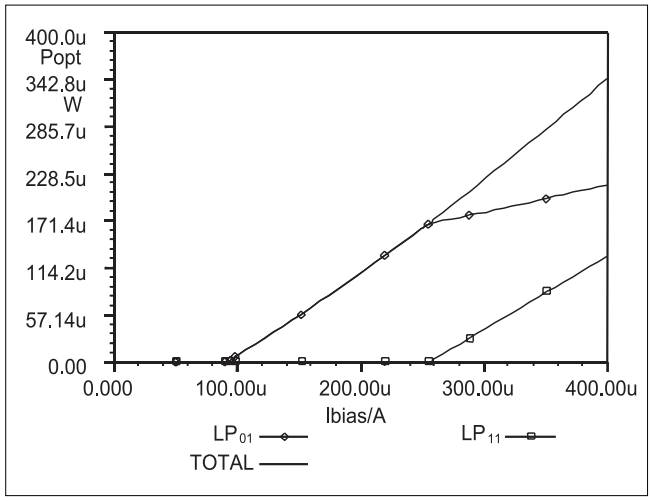

Fig. 7. Result of DC simulation, carrier distribution at I_{th} (LP_{01} starts) and $3I_{th}$ (LP_{11} starts)

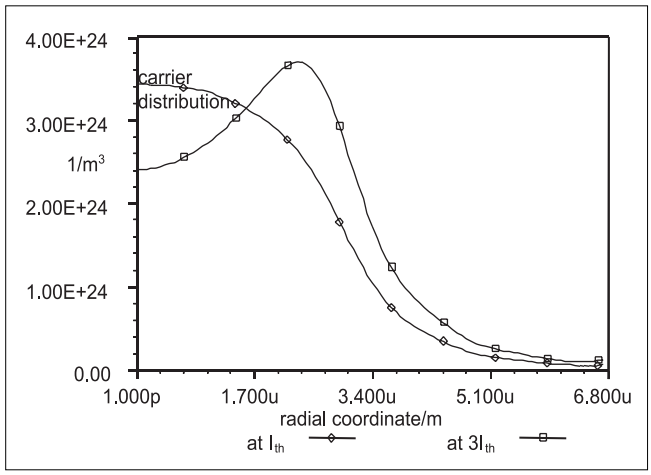

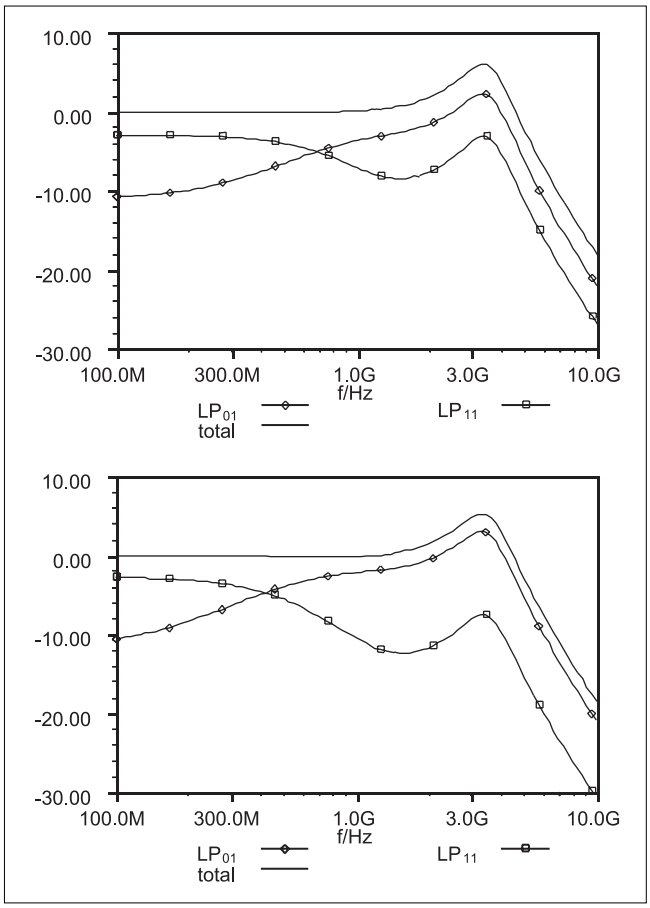

Fig.8. Results of AC simulation D=10·10^{-4} (up) and D=15·10^{-4} (bottom)

Small signal modulation characteristics, AC analysis

For the AC simulation such a bias point was chosen where both optical modes were lasing, I = 400 μA.

Fig. 8. shows the small signal modulation response for each mode and for the total intensity with two different diffusion constants. At low modulating frequency the LP_{11} mode has stronger modulation response than LP_{01}, which is a consequence of its higher slope efficiency shown by the DC simulation in Fig. 6. At high frequency the opposite becomes true, the LP_{01} mode has higher modulation response. The frequency of change depends on the diffusion constant, D, which determines how fast the diffusion can follow the modulation. In case of $D = 10 \cdot 10^{-4}$ m^2/s the characteristic frequency is around 700 MHz, while with $D = 15 \cdot 10^{-4}$ it is 450 MHz, which means that an increase in D by 3/2 times decreases the frequency to 2/3. What happens is that at higher modulation frequencies the LP_{11} mode can not gain from the diffusion process and its response to modulation decreases.

It means that the slope efficiency of the modes, which can be seen in the DC analysis, change with frequency. The total intensity does not show this change, because the carriers contribute to the stimulated emission anyway.

Distortion, harmonic balance analysis

The most interesting result of the paper is shown in *Fig. 9. and 10.*, which are the results of a single tone harmonic balance simulation. Up to the fifth harmonics of the modulating tone (at frequency f_m) was taken into account, but only the second and third harmonics are presented as most important in applications of direct modulated lasers. The amplitude of the modulating signal was $I_{bias}/10$, the bias point was $3I_{th}$. In directly modulated transmission systems the nonlinear behavior causes distortion and intermodulation. The generated second and third harmonic levels simulated here are in quantitative connection with the coefficients of the laser nonlinear characteristic and hence, have special importance.

The curves show that the laser nonlinearity increases toward the relaxation oscillation frequency in agreement with theory. It can also be seen that diffusion affects the higher order harmonics similar to the way it affects the fundamental one. The modulation response for f_m agrees with the result of the small signal (AC) analyses in Fig. 8.

Fig. 9. Harmonic balance simulation, harmonics level vs. modulating frequency

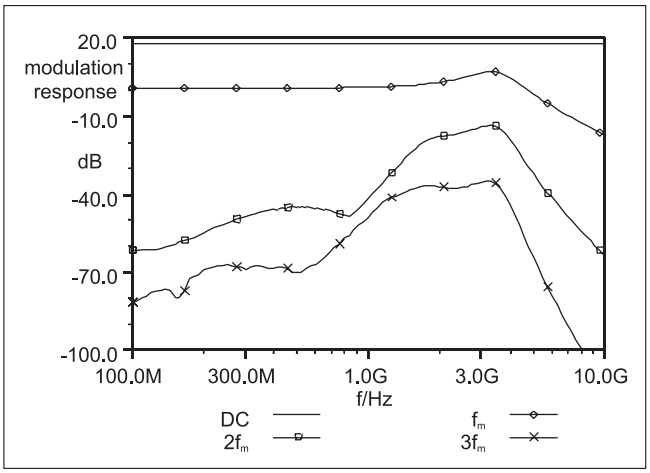

Fig. 10. Harmonic balance simulation, level of harmonics in different modes

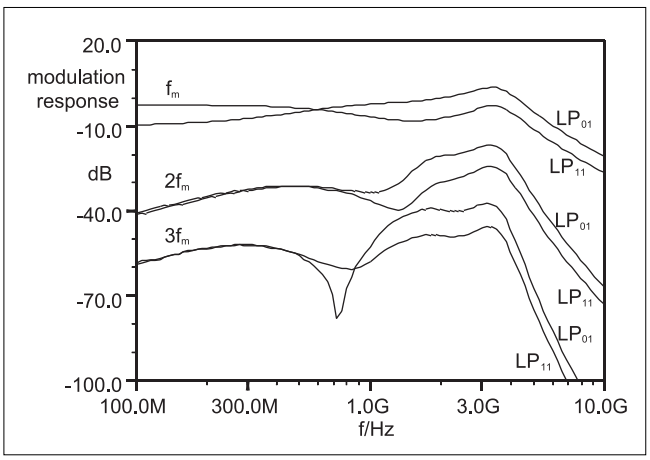

As the modulating frequency becomes higher than approximately 700 Mhz, the LP_{11} response decreases in all higher order harmonics as well. This can be important in analog application of VCSELs because external reflectivity such as a coupling fiber or a photodetector surface can enhance one mode causing the modulation proprieties to change severely. These diffusion induced modes should be avoided in properly designed VCSELs. A low optical reflection environment is needed even when these modes exist with low optical power.

Interesting observation can be done by analyzing the numbers. The curves of the second harmonic ($2f_m$) in Fig.10. start from -40dB, while in Fig. 9, where the sum of the two modes can be seen, from -60dB. This means that the intensity of the two modes at the second harmonic are in antiphase.

Similar can be found at the third harmonic, and the opposite is true for the first harmonic (at the modulating frequency). This phenomena disappears above the characteristic frequency of diffusion, and the harmonic level, or distortion, increases. Between the two regions a deep notch can be seen in the third harmonic curve of LP_{01}, which is denoted to the antiphase behavior of the two main nonlinear processes, the SHB and the relaxation oscillation [10]. This effect is a bit different with the LP_{11} mode, and therefore it appears attenuated in the total optical intensity.

Conclusion

The basic properties and characteristics of VCSELs were introduced. The evaluation of measurement results showed that these lasers can have good performance even in demanding communication applications.

A novel equivalent circuit for modeling multiple transversal mode behavior in VCSELs was also presented. Using simulation results, the effect of spatial hole burning and carrier diffusion on the static and dynamic characteristics were shown. The different modes have different linear and nonlinear modulation properties which can cause problems with mode selective optical devices.

References

[1] Marozsak, T.; Udvary, E.; Berceli, T.:
A combined optical-wireless broadband Internet access: transmission challenges,
IEEE MTT-S International Microwave Symposium Digest,
pp.997–1000, May 2001

[2] Asa Haglund et al:
Single Fundamental Mode Output Power Exceeding 6mW in VCSELs with a Shallow Surface Relief,
will be published in
IEEE Photonics Technology Letters, Febr. 2004

[3] Tamás Marozsák, Attila Kovács, Eszter Udvary, Tibor Berceli:
Direct Modulated Lasers in Radio Over Fiber Applications,
MWP2002 International Topical Meeting on Microwave Photonics, Techn. Digest,
pp.129, Japan, 2002.

[4] Christina Carlsson et al:
Analog Modulation Properties of Oxide Confined VCSELs at Microwave Frequencies,
Journal of Lightwave Technology,
vol.20, Sept. 2002

[5] C. Faulkner:
RFIC Design Challenges for WLAN and 3G Systems,
Microwave Eng.,
pp.23–28, Jan/Feb. 2003

[6] J. C. Fan et. al.:
Dynamic Range Requirements for Microcellular Personal Communication Systems Using Analog Fiber-Optic Links,
IEEE Transactions on Microwave Theory and Techniques,
vol.45, pp.1390, 1997.

[7] L.A.Coldren, S.W.Corzine:
Diode Lasers and Photonic Integrated Circuits,
Wiley & Sons Publication, 1995.

[8] K. Moriki, H. Nakahara, T. Hattori, K. Iga :
Single transverese mode condition of surface-emitting injection lasers,
Electronic Communications Japan,
Part 2, vol.71, pp.81–90, 1988.

[9] http://www.ele.kth.se/COST268/WG1/DynVCSELTask/WGExcercise2.html

[10] J.S. Gustavsson et al:
Harmonic and Intermodulation Distrotion in Oxide-Confined Vertical Cavity Surface-Emitting Lasers,
IEEE Journal of Quantum El.,
vol.39, Aug. 2003